Observation of precipitation in Mg-Al alloys by ^{25}Mg and ^{27}Al NMR

1995 J. Phys.: Condens. Matter 7 4929

(http://iopscience.iop.org/0953-8984/7/25/016)

J. Phys.: Condens. Matter 7 (1995) 4929–4937. Printed in the UK

Observation of precipitation in Mg–Al alloys by ^{25}Mg and ^{27}Al NMR

T J Bastow† and M E Smith‡

† Division of Materials Science and Technology, CSIRO, Private Bag 33, Rosebank MDC, Clayton, Victoria 3169, Australia

‡ Physics Department, University of Kent, Canterbury, Kent, UK

Received 30 November 1994, in final form 7 April 1995

Abstract. A combination of ^{25}Mg and ^{27}Al NMR has been shown to be an effective structural probe for the intermetallic phase $Mg_{17}Al_{12}$, able to detect precipitation of this phase in dilute alloys of aluminium in magnesium during age hardening, with well-resolved signals from the precipitate and the alloy. Knight shift and spin–lattice relaxation measurements for the intermetallic phase are examined for evidence of a quasigap at the Fermi surface, recently proposed as the origin for the stability of this phase.

1. Introduction

Dilute alloys of aluminium in magnesium are used increasingly in the automotive industry to reduce weight and enable vehicles to achieve lower pollution levels. The most widely used of these alloys is AZ91 (Mg–9 wt%Al–1 wt%Zn–0.3 wt%Mn) and AM60 (Mg–6 wt%Al–0.3 wt%Mn). It is possible to strengthen these alloys by age hardening. According to the phase diagram [1] the maximum solubility of aluminium in magnesium is about 10 wt% at 437 °C. At room temperature the equilibrium concentration of Al in Mg is about 2 wt%. On cooling a casting, any excess of Al precipitates out as the intermetallic phase $Mg_{17}Al_{12}$.

Narasimhan and Davenport [2] have very recently made first-principles local-density-approximation calculations on Al–Mg intermetallic compounds and have confirmed the stability $Mg_{17}Al_{12}$ phase with respect to other possible, hypothetically stable, but as yet unobserved Mg–Al compounds, namely Mg_3Al, MgAl and $MgAl_3$. Their band structure calculations for $Mg_{17}Al_{12}$ reveal a density of states ($N(E)$) curve with a quasigap, centred at the Fermi energy E_F, corresponding to a lowering from the free electron density of states by approximately 20%. Such a quasigap is thought to be responsible for the stabilization of the Al-based icosahedral quasicrystals. Narasimhan and Davenport [2] have compared $N(E)$ for $Mg_{17}Al_{12}$, which has the α-Mn structure, with $N(E)$ for the same structure with Al on all sites and the lattice constant adjusted to give the same density as for FCC Al metal. The latter has no such quasigap at E_F.

The isotope ^{25}Mg (spin $I = \frac{5}{2}$) has a natural abundance of only 10.1% and low detection sensitivity: ^{27}Al ($I = \frac{5}{2}$) is 100% abundant and has high detection sensitivity. Thus nuclear magnetic resonance (NMR) of either or both isotopes may be used to examine Mg–Al alloys and their phases. This paper reports NMR observations in a solution-treated Mg–6 wt%Al alloy and the stoichiometric intermetallic $Mg_{17}Al_{12}$.

The calculated quasigap in $N(E)$ at E_F for $Mg_{17}Al_{12}$ [2] should be reflected in the ^{25}Mg and ^{27}Al NMR as a reduction in the Knight shift (K) and an increase in the spin–lattice relaxation time T_1. A substantial reduction in K and increase in T_1 is observed in

0953-8984/95/254929+09$19.50

the Al-based icosahedral quasicrystals [3]. The measurements reported below for $Mg_{17}Al_{12}$ suggest that if a quasigap exists, it must be relatively shallow.

2. Experimental details

A reference specimen of the high purity (3N7) Mg starting material was prepared in powder form by filing. The consequent lattice defects were removed by heating the powder for 30 min at 350 °C under a backing pump vacuum. The Mg powder was mixed with fine alumina powder to isolate the particles electrically and to prevent Joule losses in the NMR probe. The Mg–Al specimens were prepared by melting together high-purity magnesium and aluminium metals at 710 °C for 10 min in an induction heater equipped with a stirrer. The alloy was then cast into a hot steel mould at 400 °C. The Mg–6 wt%Al ingot was then solution treated at 420 °C for 24 h in argon and then water quenched. A powder specimen for NMR was prepared by filing the ingot: the powder was subsequently heat treated in argon at 420 °C for 24 h (alloy No 1), and 530 °C for 1 h, to remove any deformation caused, and to ensure that the Al was in solid solution in the alloy. The powder was quenched into water. This gave a (non-conducting) oxide layer on the surface of the alloy particles which isolated the particles electrically in the NMR probe. The ingot of the intermetallic phase $Mg_{17}Al_{12}$ was homogenized by treating it at 420 °C for 48 h in argon, and furnace cooled. It was found that this ingot was very brittle and fine powder was obtained by crushing in an agate pestle and mortar. The sharpness of the NMR lines obtained subsequently indicated that the process introduced little or no deformation of the particles and the powder was not annealed. The particles were separated from electrical contact by mixing with MgO powder. The ^{25}Mg signal from the MgO did not interfere with the signal from the intermetallic, and served as an internal marker.

The NMR spectrometer used was a Bruker MSL 400, field 9.4 T, with operating frequencies 24.48 MHz for ^{25}Mg and 104.23 MHz for ^{27}Al. For ^{25}Mg the spectra in figures 1, 2(a) and 3 were taken using a static sample with an echo pulse sequence $(t)_{\phi 1}$–τ–$(t)_{\phi 2}$–τ–acq, where the pulse length t was 5 μs ($< \pi/2$), and the phases $\phi_{1,2}$ were varied according to a 16-pulse sequence given by Oldfield *et al* [4]. The ^{25}Mg MAS spectrum in figure 3(b) was taken with an MAS probe at a rotation speed of 2.75 kHz using a t–acq pulse sequence. The ^{27}Al and ^{25}Mg spin–lattice relaxation times, T_1, for the alloy and intermetallic $(\frac{1}{2}, -\frac{1}{2})$ transitions were measured by saturation recovery. In the case of the intermetallic, the ^{25}Mg magnetization recovery for each of the three lines was detected by the echo sequence given above, and the recovery for the most intense line, Mg in 24g, displayed in figure 4. The file of ten spectra required to fit the recovery with suitable accuracy took 30 h. For ^{27}Al, the spectra (figure 5) were acquired with an MAS probe at a rotation speed of 7.0 kHz and 10.5 kHz for the alloy and intermetallic specimens respectively, using a t'–acq pulse sequence with $t' = 0.75$ μs. This pulse length gave a tip angle of $< \pi/18$ and ensured that the spectra were quantitative [5]. All measurements were made at room temperature (296 K).

The ^{25}Mg spectra were referenced to the line from an aqueous solution of $MgSO_4$ at 0 ppm, while the ^{27}Al spectra were referenced to the line from the octahedral site in yttrium aluminium garnet ($Y_3Al_5O_{12}$) at 0.7 ppm; the primary reference being the $Al(H_2O)_6^{3+}$ ion at 0 ppm. The Knight shifts, chemical shifts, nuclear quadrupole parameters ($C_q = e^2qQ/h$ and η, where resolved) and the relaxation times, T_1 corresponding to the various Mg and Al sites are given in table 1.

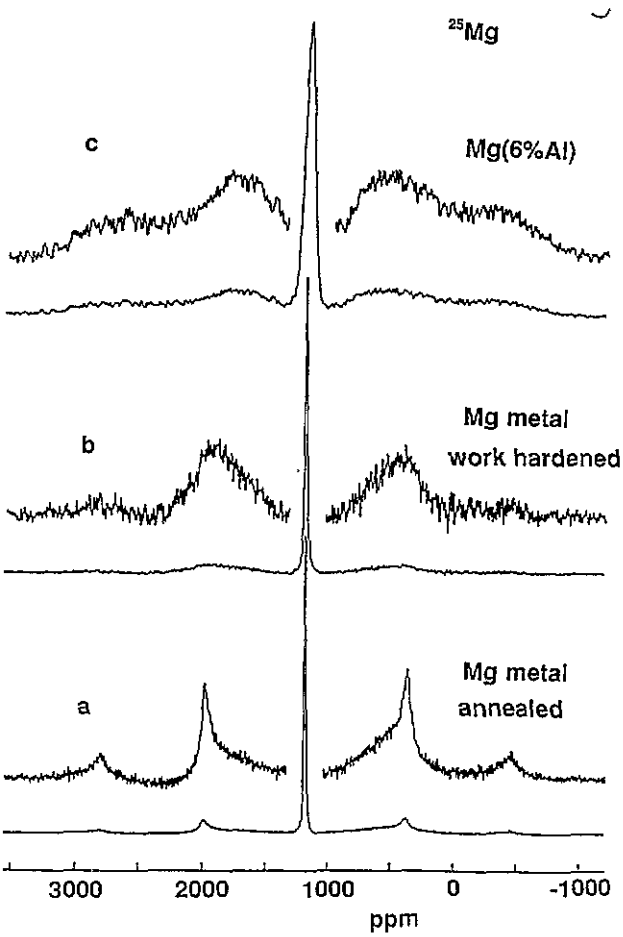

Figure 1. ^{25}Mg NMR spectrum of (a) annealed pure magnesium metal, (b) as-filed pure magnesium metal and (c) Mg(6%Al) alloy (No 1). The $\pm(\frac{3}{2}, \frac{1}{2})$ and $\pm(\frac{5}{2}, \frac{3}{2})$ satellite powder pattern features are enlarged vertically in the inset.

3. Discussion

A preliminary remark should be made about the relaxation measurements which yielded the T_1 values given in table 1. In general, for a nucleus with spin $I = \frac{5}{2}$ in a non-cubic site, (i.e. experiencing quadrupolar interaction), the $(\frac{1}{2}, -\frac{1}{2})$ magnetization, when perturbed, relaxes to equilibrium with three time constants, $(2W)^{-1}$, $(12W)^{-1}$ and $(30W)^{-1}$, where W is the $\Delta m = \pm 1$ magnetic relaxation transition probability. It is assumed here that all relaxation is magnetic, i.e. that quadrupolar, and especially dipolar [6], contributions are negligible. After *complete* saturation of $(\frac{1}{2}, -\frac{1}{2})$ and *all* satellite transitions, the $(\frac{1}{2}, -\frac{1}{2})$ magnetization recovers with a single relaxation time $T_1 = (2W)^{-1}$, independent of the magnitude of the quadrupolar interaction [6]. If saturation is incomplete, then the two faster time constants will also contribute. In all cases encountered here, except for ^{25}Mg in $Mg_{17}Al_{12}$ which is discussed further below, the saturation appeared complete and the magnetization recoveries were excellently fitted by a single relaxation time assumed to be $(2W)^{-1}$.

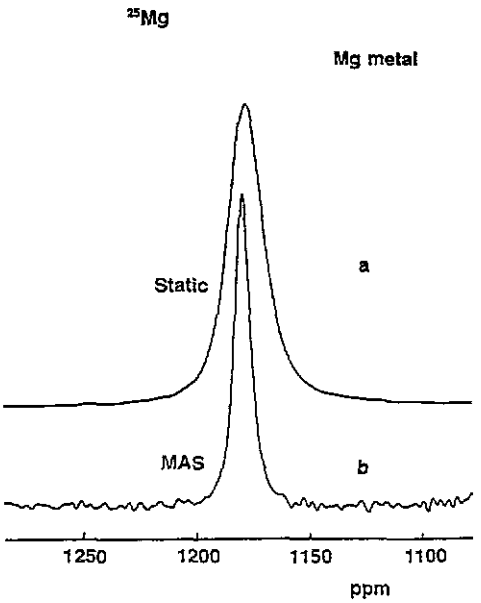

Figure 2. Comparison between (a) static and (b) MAS ^{25}Mg NMR lineshapes for pure annealed magnesium.

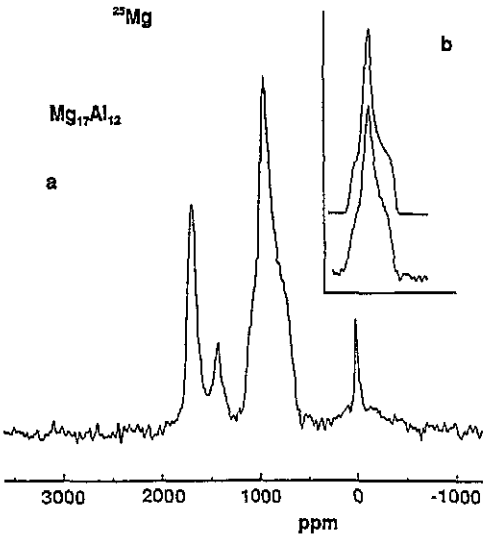

Figure 3. ^{25}Mg NMR spectrum of the $Mg_{17}Al_{12}$ intermetallic specimen, showing (a) the $(\frac{1}{2}, -\frac{1}{2})$ lines from the three inequivalent Mg sites (from left to right, 8c, 2a and 24g) and also the line from the MgO at 24 ppm, and (b) a comparison of the simulated (above) and experimental (below) lineshapes for Mg in position 24(g). The frequency axis is expanded relative to figure 2(a).

^{25}Mg

The nuclear quadrupole perturbed spectrum for ^{25}Mg in polycrystalline HCP magnesium metal has been reported previously [7], along with the temperature dependence of the nuclear quadrupole interaction (C_Q), the spin–lattice relaxation time (T_1) and the Knight shift (K). The value of K (proportional to $N(E_F)$) is linked to the value of T_1 by the Korringa relation [8]. In the free-electron approximation, this takes the form

$$T_1 K^2 = \left(\hbar/4\pi k_B T\right)\left(\gamma_e/\gamma_n\right)^2 \tag{1}$$

where γ_e and γ_n are the gyromagnetic ratios for the electron and nucleus respectively. The derivation of this expression is based on the assumption that the sole relaxing process is magnetic and due to the contact interaction between electron and nucleus (which also gives rise to the Knight shift). If, for example, the quadrupole interaction contributed appreciably to the relaxation there would be a T^{-2} contribution due to indirect phonon Raman processes [9]. It should be noted that the observed temperature dependence for ^{25}Mg in Mg metal is $T_1 \propto T$ to within experimental accuracy [7].

The contribution from the ^{25}Mg nuclear dipole–dipole interaction (assuming Gaussian lineshape) and the measured quadrupole interaction (C_q = 266 kHz) to the $(\frac{1}{2}, -\frac{1}{2})$ linewidth (FWHM) for pure annealed Mg can be easily calculated to be 89 Hz and 91 Hz respectively. The observed linewidth in the annealed metal (figure 1(a)) is 450 Hz which was initially attributed predominantly to Knight shift anisotropy. However, an MAS spectrum

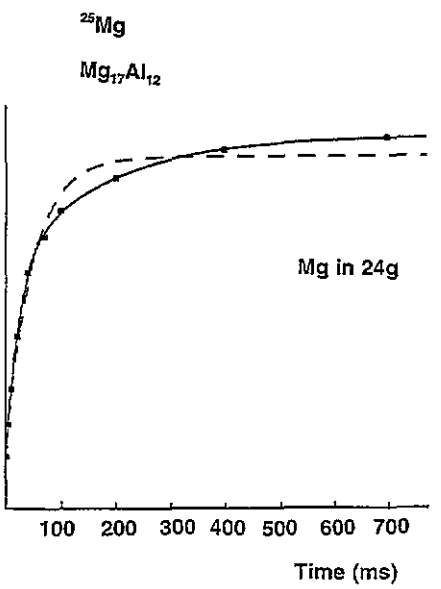

Figure 4. ^{25}Mg magnetization recovery in $Mg_{17}Al_{12}$ after a 16×8 μs pulse saturation sequence, showing the best fit to data (■) for one time constant (dashed line) and two time constants (full line). The two relaxation time constants for the full line fit were 171 μs and 23 μs respectively; the ratio of the two identifies the longer time as $(2W)^{-1}$.

for this material (figure 2(b)) displayed a linewidth of 200 Hz, instead of approximately 30 Hz which is that part (roughly a third) of the second-order quadrupolar interaction not removed by MAS. Since independent contributions add in quadrature to the second moment, almost all of this MAS linewidth must have its origins in unannealed defects as discussed in the following paragraph. From figure 2 it may be seen that the MAS line is displaced by about 1 ppm to a higher frequency with respect to the static line. The lines were carefully referenced immediately after acquisition, so the shift is probably real and may be due to the axial Knight shift. Of the 250 Hz that was removed from the static FWHM linewidth by MAS, approximately 90 Hz can be accounted for as dipolar and 60 Hz as second-order quadrupolar. This leaves approximately 225 Hz (i.e. $(250^2 - 90^2 - 60^2)^{1/2}) = 9$ ppm as an upper limit for the Knight shift anisotropy contribution. According to the conventional definition [10], this gives $K_{ax} \leqslant 9/3 \approx 3$ ppm. This is of the order of the value 2(1) ppm suggested by previous single-crystal work [11].

The lattice defects introduced by filing increased the width of the central $(\frac{1}{2}, -\frac{1}{2})$ transition by about 20%, from 450 Hz in the annealed state to 550 Hz in the deformed state, and simultaneously lowered the frequency of the transition by about 3–4 ppm (figure 1(b)). The first order $\theta = 90°$ powder singularities from the satellite transitions are heavily smeared in figure 1(b), but are still discernible. The defects generate a distribution of electric field gradients giving a $\delta\nu_q$ around the mean value for the annealed material (where $\nu_q = 20C_q/3$). This smears the satellite singularities around positions determined by $\nu_{q,mean}$ by an amount proportional to $\delta\nu_q$, but contributes an additional width to the $(\frac{1}{2}, -\frac{1}{2})$ line of $2\nu_q(\delta\nu_q)/\nu_L$, where ν_L is the Larmor frequency. A reasonable estimate of the satellite smearing from figure 1(b) of $\delta\nu_q = 400$ ppm (= 10 kHz) yields a value for the additional width of 110 Hz which is close to the observed increase in the $(\frac{1}{2}, -\frac{1}{2})$ linewidth of $(550 - 450) = 100$ Hz.

From the ^{25}Mg spectrum (figure 1(c)) it may be inferred that the Mg–6 wt%Al alloy

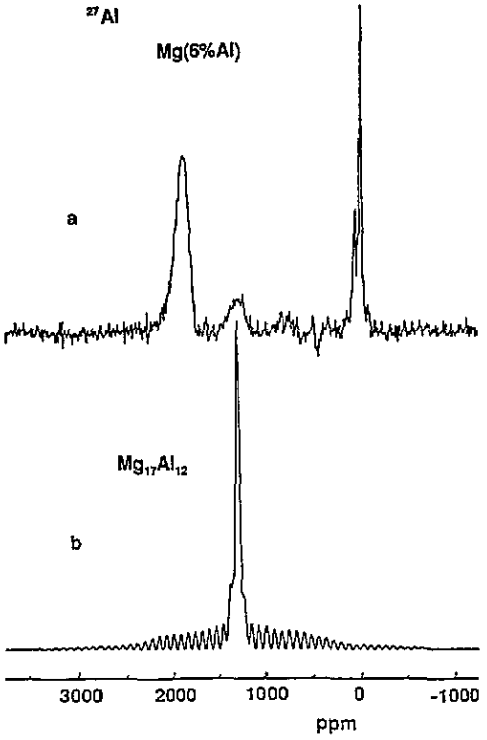

Figure 5. ^{27}Al MAS NMR spectra of (a) the Mg(6%Al) alloy (No 2), showing the $(\frac{1}{2}, -\frac{1}{2})$ lines from the solid solution phase (1882 ppm), the intermetallic precipitate (ca. 1300 ppm) and the $MgAl_2O_4$ surface layers (8 and 64 ppm) on the metal particles, (b) the single $(\frac{1}{2}, -\frac{1}{2})$ line for the $Mg_{17}Al_{12}$ intermetallic phase, centred in the spinning sideband pattern due to the satellite transitions.

(No 1) resembles, apart from some substitutional disorder, the unperturbed magnesium HCP structure. The similar Knight shift K, quadrupole coupling constant C_q and spin–lattice relaxation time T_1 (table 1) indicate no remarkable departure from the electronic structure of Mg, as might be expected. The Korringa product T_1K^2T is given in table 2. The ^{25}Mg spectrum for alloy No 1, figure 1(c), shows the central $(\frac{1}{2}, -\frac{1}{2})$ line with a Knight shift about 16 ppm less than for pure magnesium, and a width of 2.3 kHz, an increase by a factor of five over that for pure magnesium. This line was not narrowed by MAS at 3.45 kHz. The satellite singularities are smeared out, but still resolved, and indicate a C_q for the alloy reduced by about 15% with respect to pure magnesium (figure 1(c), table 1). Since alloying with 6% aluminium is observed to *decrease* C_q, the fivefold increase in the $(\frac{1}{2}, -\frac{1}{2})$ linewidth must be due to a distribution of the local, predominantly isotropic, Knight (or chemical) shifts associated with the Al substitutions. No other ^{25}Mg lines are visible at this level of signal to noise.

The ^{25}Mg spectrum of the intermetallic, figure 3(a), is qualitatively different from that of the alloy. The published crystal structure [12] indicates a unit cell containing three distinct Mg sites with Mg in positions 2a (43m), 8c (3m) and 24g (m), where the site symmetry is indicated in brackets. A three line NMR spectrum is therefore expected with integrated intensities in the ratio 1:4:12. A three-line spectrum is indeed observed (the line at 24 ppm shift is from the MgO) with intensities in the ratio 1.1:3.6:12 which is strikingly close to that expected. These lines are the central $(\frac{1}{2}, -\frac{1}{2})$ transitions corresponding to the three sites; the

Table 1. NMR parameters for ^{25}Mg and ^{27}Al in the Mg–Al system.

Material	Nucleus	Knight shift (%)	C_q (MHz); η 296 K	T_1 (ms)[a] (= $[2W]^{-1}$)
Al (metal)	^{26}Al	0.1640(1)	—; 0	6.3
Mg (metal)	^{25}Mg	0.1179(1)	0.266(1); 0	245
Mg(6%Al)	^{25}Mg	0.1163(2)	0.226(10); 0	210
	^{27}Al	0.1890(5)	< 2.3[b]; 0	5.1
		0.130[c]		nm
		0.0008[d]		nm
		0.0064[e]		nm
$Mg_{17}Al_{12}$	^{25}Mg 24g	0.0990	2.20; 0.95	171
	2a	0.1445	0; 0	88
	8c	0.1705	< 1.2[b]; ≈0	84
		0.0024[f]	0	nm
	^{27}Al	0.1300(5)	0.72	8.7

[a] T_1 measured at 296 K.
[b] Calculated assuming FWHM to be quadrupolar in origin, and $\eta = 0$.
[c] $Mg_{17}Al_{12}$ precipitate.
[d] $MgAl_2O_4$—octahedral site.
[e] $MgAl_2O_4$—tetrahedral site.
[f] MgO.

Table 2. Korringa product for ^{25}Mg and ^{27}Al in the Mg–Al system.

	T_1TK^2 (T = 296 K)	
	^{25}Mg (10^{-5} sK)	^{27}Al (10^{-6} sK)
Free electrons[a]	7.02	3.87
Al metal	—	4.98
Mg metal	10.0	—
Mg_6Al	8.41	5.34
$Mg_{17}Al_{12}$	(24 g) 4.09	4.33
	(8a) 5.44	
	(2a) 7.23	

[a] For free electrons $T_1TK^2 = (\hbar/4\pi k_B)(\gamma_e/\gamma_n)^2$.

satellite transitions are not observed. Note that the powder for the $Mg_{17}Al_{12}$ specimen was obtained by crushing the ingot without further annealing, although a well-defined spectrum was obtained, as can be seen in figure 3(a). However, there will inevitably be lattice defects present contributing a distribution of electric field gradients which will disperse the satellite contributions from Mg in 8a, and even the cubic site Mg in 2a, leaving only the $(\frac{1}{2}, -\frac{1}{2})$ contribution sharply defined. It may also be noted that in a static spectrum (unlike an MAS spectrum) the $(\frac{1}{2}, -\frac{1}{2})$ line intensity is strictly proportional to the number of contributing sites, independent of the magnitude of the coupling constant.

The line from Mg in position 24g has quadrupolar structure from which the coupling constant and asymmetry parameter may be obtained. A simulation using the Bruker program POWDER yielded the values for δ_{iso} (= K), C_q and η given in table 1. The simulated and observed line shape are compared in figure 3(b). The line from Mg in 8c should have $\eta = 0$ since there is axial symmetry (3m), and the narrowness of the line indicates a small C_q. The line from Mg in 2a should have $C_q = 0$ since the site symmetry is cubic (43m). The line from the MgO reference near zero is well separated from the metal lines. The considerable

dispersion in Knight shift for the three sites reflects their differing partial density of states at the Fermi surface $N(E_F, i)$, where i = 2a, 8c and 24g, from the Mg 3s electrons with a suitable admixture of Al 3s and 3p. This could be checked in principle by a suitably detailed band structure calculation.

The ^{25}Mg relaxation to equilibrium after a saturation sequence was multi-exponential for Mg in 24g and 8c in the intermetallic, reflecting the difficulty in saturating the satellite transitions in the presence of sufficiently large quadrupole interactions, as discussed above. Although the fit to one exponential was poor for these two sites, the fit to two exponentials was sufficiently good to make the fitting of a possible third (shorter) time constant indeterminate with the present data. For Mg in 24g, for which the recovery after approximately 90% saturation is shown in figure 4, the longer of the two resolved time constants is assumed to be $(2W)^{-1}$. The other is a factor approximately seven shorter, which compares reasonably satisfactorily to a theoretical factor of six. A very similar analysis was made for Mg in 8c. For Mg in 2a, the relaxation was fitted well with only one time constant, presumably due to its formal cubic point symmetry and consequent greater ease of saturation. The Korringa products listed in table 2 indicate a systematic difference between the three sites, but no severe differences from the free-electron or metallic Mg values. The greatest departure is for Mg in 24g.

^{27}Al

The ^{27}Al MAS spectrum for alloy No 2, figure 5(a), shows a number of Al signals, all $(\frac{1}{2}, -\frac{1}{2})$ transitions. The most intense line at 1882 ppm is from the host alloy phase. The narrow lines with shifts 8 and 64 ppm are due to the octahedral and tetrahedral (inversion) sites respectively of $MgAl_2O_4$ spinel [5], which is formed during the annealing process. Note that the line narrowing from MAS separates the octahedral and tetrahedral lines and enables such a precise identification to be made. The line at 1300 ppm is the $(\frac{1}{2}, -\frac{1}{2})$ transition from the intermetallic phase (table 1 and below). The presence of this indicates that the powder specimen of the alloy Mg–6 wt%Al was imperfectly quenched, and some of the intermetallic phase $Mg_{17}Al_{12}$ remained. From a measurement of the relative intensities, it can be estimated that the specimen contains just under 3 wt% $Mg_{17}Al_{12}$. The width of the resonance at 1882 ppm suggest a relatively well-defined Al environment, consistent with the great majority of Al atoms having all Mg nearest neighbours, but one which is distinctly different from Al in metallic aluminium or the intermetallic phase, as shown in the ^{27}Al Knight shifts (table 1 and below). The Korringa product T_1K^2T for this site (table 2) is close to the free-electron value for aluminium metal.

The well-ordered $Mg_{17}Al_{12}$ intermetallic specimen yielded an MAS spectrum (figure 5(b)) from which both C_q and η could be extracted. Only one site is observed, consistent with the crystal structure [12] which has all Al atoms in positions 24g (m). The central $(\frac{1}{2}, -\frac{1}{2})$ line is narrow and featureless, but the nuclear quadrupole parameters can be obtained from the spinning sideband pattern which traces out the static first-order quadrupole-perturbed powder spectrum. In fact, a reasonable value for C_q can be obtained immediately from the frequency separation of the well-defined outer limits of the sideband pattern, which yields $4\nu_Q = 3C_q/5 = 480$ kHz. A more accurate estimate for C_q, together with a value for η, can be obtained by simulation of the whole powder pattern, and the values are given in table 1. The position of the strong central line identifies the low intensity peak in the alloy spectrum (figure 5(a)) as due to precipitates of the intermetallic phase. The Korringa product (table 2) for the site is between the values for free electrons and aluminium metal.

4. Conclusions

The fact that ^{25}Mg quadrupolar details persist in the satellite lineshape of the 6%Al alloy is surprising, reflecting the relatively small quadrupole interaction of ^{25}Mg. Also surprising is the clearly resolved detail in the ^{25}Mg spectrum by which one can observe the three Mg sites in the intermetallic compound. This appears to be due not just to the Knight shift dispersion, but also to the brittleness of the material, in that it fractures on crushing without plastic deformation, thus maintaining the crystal perfection of the homogenized ingot. Detailed spectra, useful for materials characterization, can be obtained without the need for magic angle spinning.

The ^{27}Al spectrum of the dilute alloy demonstrates that, because of high detection sensitivity and Knight shift dispersion, the low level of Al in the host solid solution can be detected and resolved from the even lower level of aluminium present in the precipitated intermetallic phase with good signal to noise ratio. In a further series of experiments [13] it has been shown, *inter alia*, that levels of 0.25 wt% Al in Mg metal can be easily detected. Furthermore, judicious use of MAS for this isotope can yield useful impurity-phase content and quadrupolar details that are obscured in a static spectrum. The relatively small departure of the Korringa products from the free-electron or the elemental constituent values suggest that if there exists a quasigap in $N(E)$ at E_F it must be relatively shallow (which would be consistent with the predictions in [2]), and then possibly associated with electron states centred on Mg in 24g.

Acknowledgments

We would like to thank P Humble, C Bettles and J Nie for supplying the specimens, for tuition in elementary metallurgy and for many useful suggestions. We are grateful to S N Stuart for a critical reading of the manuscript.

References

[1] Nayeb-Hashemi A A and Clark J B (ed) 1988 *Phase Diagrams of Binary Magnesium Alloys* (Metals Park, OH: ASM International)
[2] Narasimhan S and Davenport J W 1995 *Phys. Rev.* B **51** 659
[3] Shastri A, Borsa F, Torgeson D R, Shield J E and Goldman A I 1994 *Phys. Rev.* B **50** 15 651 and references therein
[4] Kunwar A C, Turner G L and Oldfield E 1986 *J. Mag. Res.* **69** 124
[5] Smith M E 1992 *Appl. Mag. Res.* **4** 1
[6] Narath A 1967 *Phys. Rev.* **162** 320
[7] Bastow T J 1991 *J. Phys.: Condens. Matter* **3** 753–6
[8] Winter J 1971 *Magnetic Resonance in Metals* (Oxford: Oxford University Press)
[9] Abragam A 1961 *Principles of Nuclear Magnetism* (Oxford: Oxford University Press)
[10] Carter G C, Bennett L H and Kahan D J 1977 *Metallic Shifts in NMR, Part I* (Oxford: Pergamon)
[11] Dougan P D, Sharma S N and Williams D L 1969 *Can. J. Phys.* **47** 1047
[12] Schobinger-Papamentellos P and Fischer P 1970 *Naturwiss.* **57** 128
[13] Bastow T J and Celotto S 1995 unpublished